Am J Physiol Gastrointest Liver Physiol 317: G453–G462, 2019.
First published August 14, 2019; doi:10.1152/ajpgi.00103.2019.

RESEARCH ARTICLE | *Inflammation, Immunity, Fibrosis, and Infection*

High-fat diet promotes experimental colitis by inducing oxidative stress in the colon

Xue Li,[1] Xinzhi Wei,[1] Yue Sun,[1] Jie Du,[2] Xin Li,[1] Zhe Xun,[1] and Yan Chun Li[2]

[1]*Institute of Health Sciences, China Medical University, Shenyang, Liaoning, China; and* [2]*Department of Medicine, Division of Biological Sciences, The University of Chicago, Chicago, Illinois*

Submitted 16 April 2019; accepted in final form 6 August 2019

Li X, Wei X, Sun Y, Du J, Li X, Xun Z, Li YC. High-fat diet promotes experimental colitis by inducing oxidative stress in the colon. *Am J Physiol Gastrointest Liver Physiol* 317: G453–G462, 2019. First published August 14, 2019; doi:10.1152/ajpgi.00103.2019.—Diets high in animal fats are associated with increased risks of inflammatory bowel disease, but the mechanism remains unclear. In this study, we investigated the effect of high-fat diet (HFD) on the development of experimental colitis in mice. Relative to mice fed low-fat diet (LFD), HFD feeding for 4 wk increased the levels of triglyceride, cholesterol, and free fatty acids in the plasma as well as within the colonic mucosa. In an experimental colitis model induced by 2,4,6-trinitrobenzenesulfonic acid (TNBS), mice on 4-wk HFD exhibited more severe colonic inflammation and developed more severe colitis compared with the LFD counterparts. HFD feeding resulted in higher production of mucosal pro-inflammatory cytokines, greater activation of the myosin light chain kinase (MLCK) tight junction regulatory pathway, and greater increases in mucosal barrier permeability in mice following TNBS induction. HFD feeding also induced gp91, an NADPH oxidase subunit, and promoted reactive oxygen species (ROS) production in both colonic epithelial cells and lamina propria cells. In HCT116 cell culture, palmitic acid or palmitic acid and TNF-α combination markedly increased ROS production and induced the MLCK pathway, and these effects were markedly diminished in the presence of a ROS scavenger. Taken together, these data suggest that HFD promotes colitis by aggravating mucosal oxidative stress, which rapidly drives mucosal inflammation and increases intestinal mucosal barrier permeability.

NEW & NOTEWORTHY This study demonstrates high-fat diet feeding promotes colitis in a 2,4,6-trinitrobenzenesulfonic acid-induced experimental colitis model in mice. The underlying mechanism is that high-fat diet induces oxidative stress in the colonic mucosa, which increases colonic epithelial barrier permeability and drives colonic mucosal inflammation. These observations provide molecular evidence that diets high in saturated fats are detrimental to patients with inflammatory bowel diseases.

colitis; high-fat diet; intestinal epithelial barrier; oxidative stress

INTRODUCTION

As a major disorder of the gastrointestinal tract in humans, inflammatory bowel disease (IBD), including ulcerative colitis (UC) and Crohn's disease (CD), has no clear etiology (13), but it is generally accepted that inappropriate activation of the intestinal mucosal immune system is a primary contributor to this disorder (30). The mucosal epithelial barrier plays a key role in the protection against mucosal inflammation and in the maintenance of the homeostasis of the intestinal tract, as it separates luminal bacteria, toxins, and antigens from the mucosal immune system (19, 42). Dysfunction of the barrier usually leads to increased barrier permeability and thus invasion of luminal antigens and bacteria into the lamina propria, triggering immune cell-mediated mucosal inflammation (11, 13). Indeed, increased permeability of the mucosal barrier has been well documented in patients with IBD (34). The tight junction seals the intercellular space of intestinal epithelial cells and regulates the permeability of the epithelial barrier. Myosin light chain kinase (MLCK) is a key regulator of tight junction permeability (8, 17). MLCK phosphorylates myosin II regulatory light chain (MLC), which leads to remodeling of the tight junction structure (36). It is well known that inflammatory mediators, such as pro-inflammatory cytokines, are able to disrupt epithelial tight junctions. Pro-inflammatory cytokines, such as TNF-α, highly induces MLCK expression to promote tight junction dysregulation (9, 41). Moreover, tight junctions can also be compromised by oxidative stress (12, 32), which may be involved in tyrosine kinase-mediated tight junction protein phosphorylation (25, 31). It is well known that there is a close link between oxidative stress and inflammation in cancer development (33); therefore, it is conceivable that oxidative stress can also disrupt epithelial tight junctions via inducing inflammation.

Dietary effects on the onset and development of IBD have been an interesting topic in IBD research (18). Diets can trigger IBD or have therapeutic effects on colitis (20). For example, long-term intake of dietary fats is associated with the risk of IBD: high intake of dietary long-chain n-3 polyunsaturated fats may be associated with a reduced risk of UC, whereas high intake of trans-unsaturated fats may be associated with an increased risk of UC (1). Western diets, high in saturated fats and sucrose and low in fibers, may present a risk factor for increased mucosal inflammation and IBD (38). Indeed, a high-fat diet (HFD) has been reported to exacerbate the development of experimental colitis in various experimental models, and the promoting effect was thought to be independent of obesity (14, 27, 40). However, the exact mechanism underlying the damaging effect of HFD remains to be clarified. In this report, we presented strong evidence that HFD promotes experimental colitis by inducing mucosal oxidative stress leading to increases in mucosal barrier permeability.

Address for reprint requests and other correspondence: Y. C. Li, Dept. of Medicine, The University of Chicago, 900 E. 57th St., KCBD 9110, Chicago, IL 60637 (e-mail: cyan@medicine.bsd.uchicago.edu).

Table 1. *Nucleotide sequences of PCR primers used in the study*

Primer Name	Forward (5′-3′)	Reverse (5′-3′)
mTNF-α	TCAGCCTCTTCTCATTCCTG	CAGGCTTGTCACTCGAATTT
mIL-1β	GAAATGCCACCTTTTGACAGTG	TGGATGCTCTCATCAGGACAG
mIL-6	ATAGTCCTTCCTACCCCAATTTCC	CTGACCACAGTGAGGAATGTCCAC
mIFN-γ	GCGTCATTGAATCACACCTG	TGAGCTCATTGAATGCTTGG
mIL-17	TCCCTCTGTGATCTGGGAAG	AGCATCTTCTCGACCCTGAA
mIL-23p19	AATAATGTGCCCCGTATCCA	CATGGGGCTATCAGGGAGTA
mMCP-1	CAAGAAGGAATGGGTCCAGA	TGAGGTGGTTGTGGAAAAGG
mGAPDH	TGTGTCCGTCGTGGATCTGA	CCTGCTTCACCACCTTCTTGA

METHODS

Animals and treatment. Male C57BL/6 mice (6–8 wk old, 18–20 g) were housed under a 12-h light/dark cycle at room temperature with ad libitum access to food and water. The mice were either fed an HFD (TP-23520, Trophic Diet, China), which contained 60% available energy as fat, or a low-fat diet (LFD; TP-23524, Trophic Diet, China), which contained 10% available energy as fat, for 4 wk. After 4 wk dietary treatment, experimental colitis was induced using 2,4,6-trinitrobenzenesulfonic acid (TNBS; Sigma-Aldrich), according to a protocol previously described (45). Briefly, mice were presensitized with 1% TNBS solution; after 8 days, mice that had been fasted overnight were treated under anesthesia with 0.1 mL of solution consisting of 5%TNBS and 100% alcohol (1:1) via intrarectal injection. Control mice received 50% alcohol treatment. Body weight, stool consistency, and rectal bleeding were monitored daily. Mice were usually killed on the third day after TNBS treatment, and colons were harvested immediately for histological and biochemical analyses. Clinical scores were assessed as detailed previously (37). Colonic mucosa was scraped to isolate total RNAs or proteins. All animal studies were approved by the Institutional Ethical Committee of China Medical University.

Assessment of lipids. Mouse blood and colon were collected after 4 wk of dietary treatment for lipid measurement. Colonic mucosal lipids were extracted using a mixture of chloroform and methanol according to a rapid lipid extraction method described previously (3). The extracted lipids were naturally dried and weighed. Triglyceride, cholesterol, and nonesterified free fatty acid contents were quantified using commercial assay kits purchased from Nanjing Jiancheng Bioengineering Institute, China, according to the manufacturer's instructions.

Measurement of colonic permeability. To measure colonic mucosal permeability in vivo, mice were fasted for 6 h before being gavaged with 4,000 Da FITC-dextran at 200 mg/kg as described (9). After 2 h, blood was collected, and serum FITC-dextran content was determined using an M200 TECAN microplate reader at 530 nm wavelength. To measure transepithelial electrical resistance (TER) of the colon, 1.5 cm of distal colon was mounted onto the Ussing chamber system (Physiologic Instruments, San Diego, CA), and TER was recorded as reported previously (22).

Histological analysis and immunofluorescence staining. The colon was collected from mice immediately after death, fixed overnight in 4% formaldehyde made in PBS (pH 7.2–7.4), processed, and embedded in paraffin wax. Colons were embedded as "Swiss roll" as described (29). Tissue blocks were cut into 4-μm sections and stained with hematoxylin and eosin for examination. Colonic histologic scores were recorded according to a previously described scoring system (2, 16). For immunostaining, antigen retrieval was carried out using high-pressure cooking in 10 mM sodium citrate buffer. Slides were blocked for 30 min at room temperature with 5% goat serum, followed by incubation with anti-ZO-1 antibody (66452-1-lg, Proteintech) overnight at 4°C and then with DyLight-488-conjugated secondary antibody (E-032210, EarthOx) for 1 h at room temperature. The slides were also costained with 4′,6-diamidino-2-phenylindole (C-0060, Solarbio) for 10 min before being examined under a Leica fluorescence microscope.

Electronic microscopy. Colon tissue pieces were fixed in 2.5% glutaraldehyde and postfixed in 1% osmium tetroxide. Fixed colon tissues were dehydrated through graded alcohols, penetrated with acetone, and embedded in epoxy resin. Ultrathin pieces (70–90 nm) were stained with uranyl acetate and lead citrate and then examined under a Hitachi H7650 electron microscope (Tokyo, Japan). Measurement of mitochondrial diameter (width) and length were based on at least three electronic microscopic micrographs and four to six cells.

Cell culture and treatment. HCT116 cells were cultured in RPMI 1640 medium supplemented with 10% fetal bovine serum at 37°C and 5% CO_2. Cells were treated with 100 ng/mL TNF-α, 100 μM palmitic acid (PA), or both for 12 h. In some experiments, the cells were

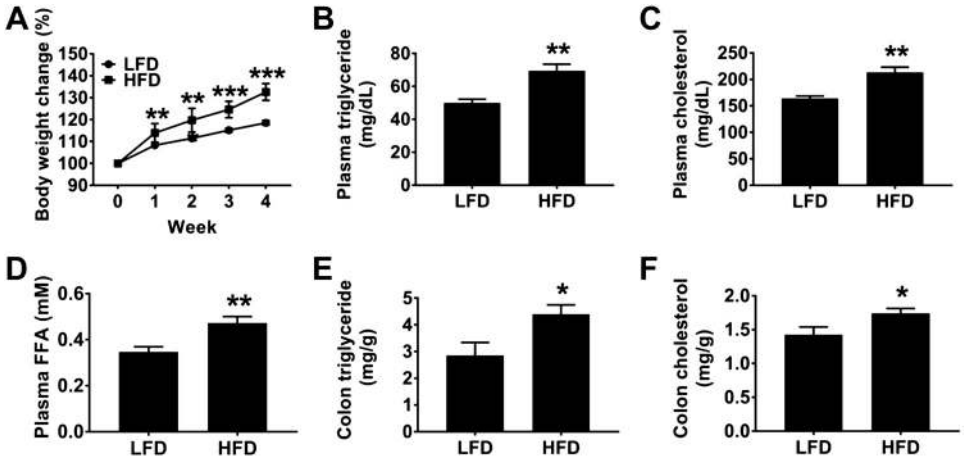

Fig. 1. High-fat diet (HFD) feeding increases lipid contents in the plasma and colonic mucosa. Body weight changes in mice on low-fat diet (LFD) or HFD for 4 wk (*A*). $^{**}P < 0.01$, $^{***}P < 0.001$ vs. LFD; $n = 9$ each group. Triglyceride (*B*), cholesterol (*C*), and free fatty acid (FFA; *D*) content in the plasma of LFD-fed or HFD-fed mice. $^{**}P < 0.01$ vs. LFD; $n = 10$–12 each group. Triglyceride (*E*) and cholesterol (*F*) content in colonic mucosa of LFD-fed or HFD-fed mice. $^{*}P < 0.05$ vs. LFD; $n = 8$ each group.

pretreated with 5 mM *N*-acetyl-L-cysteine (NAC; A-9165, Sigma-Aldrich) for 1 h before these treatments.

Measurement of reactive oxygen species. To measure reactive oxygen species (ROS) in colonic epithelial cells and lamina propria cells, colons were opened longitudinally, washed in cold PBS, and cut into 2-cm pieces. The pieces were incubated twice in HBSS containing 5 mM EDTA and 1 mM DTT for 20 min at 37°C. The supernatant was collected and centrifuged for 5 min at 1,500 revolutions/min to collect colonic epithelial cells. Then the tissues were digested in RPMI 1640 medium supplemented with 20% fetal bovine serum containing collagenase VIII (200 U/mL, Sigma-Aldrich) and DNaseI (50 U/mL, Sigma-Aldrich) for 1.5 h at 37°C. The supernatant was centrifuged at 1,500 revolutions/min for 5 min to harvest colonic lamina propria cells (15, 44). ROS was measured using a Reactive Oxygen Species Assay kit (S-0033, Beyotime) according to the manufacturer's instruction. The epithelial and lamina propria cells were resuspended in serum-free RPMI 1640 medium and loaded with 10 μM 2′,7′-dichlorodihydrofluorescein diacetate for 30 min at 37°C and 5% CO_2. After two washes with PBS, the cells were observed under a Leica inverted fluorescence microscope. Similarly, HCT116 cells were loaded with 10 μM 2′,7′-dichlorodihydrofluorescein diacetate for 30 min at 37°C and 5% CO_2, washed twice with PBS, and observed under a Leica fluorescence microscope.

Measurement of mitochondrial membrane potential. Mitochondrial membrane potential was assessed using a commercial JC-1 Mitochondrial Membrane Potential Assay kit (C-2006, Beyotime) according to the manufacturer's protocol. Tetraethylbenzimidazolylcarbocyanine iodide (JC-1)-stained cells were analyzed by flow cytometry. JC-1 is a cationic dye that accumulates in energized mitochondria. At low concentrations (due to low mitochondrial membrane potential), JC-1 is predominantly a monomer that yields green fluorescence with emission of 530 ± 15 nm. At high concentrations (because of high mitochondrial membrane potential), the dye aggregates, yielding a red to orange color with emission of 590 ± 17.5 nm (4). The polarization of mitochondrial membranes was expressed as red fluorescence to green fluorescence ratio.

Western blot analysis. Proteins were separated on SDS-PAGE, transferred to polyvinylidene fluoride (PVDF) membranes and blotted with primary antibodies, followed by appropriate secondary antibodies and chemiluminescent detection, as reported previously (21). The primary antibodies used in this study were against β-actin (sc-47778, Santa Cruz Biotechnology), TNF-α (ab-9739, Abcam), p-MLC (3674, Cell Signaling), MLCK (ab-76092, Abcam), occludin (ab-216327, Abcam), claudin-2 (ab-53032, Abcam), and gp91 (ab-129068, Abcam).

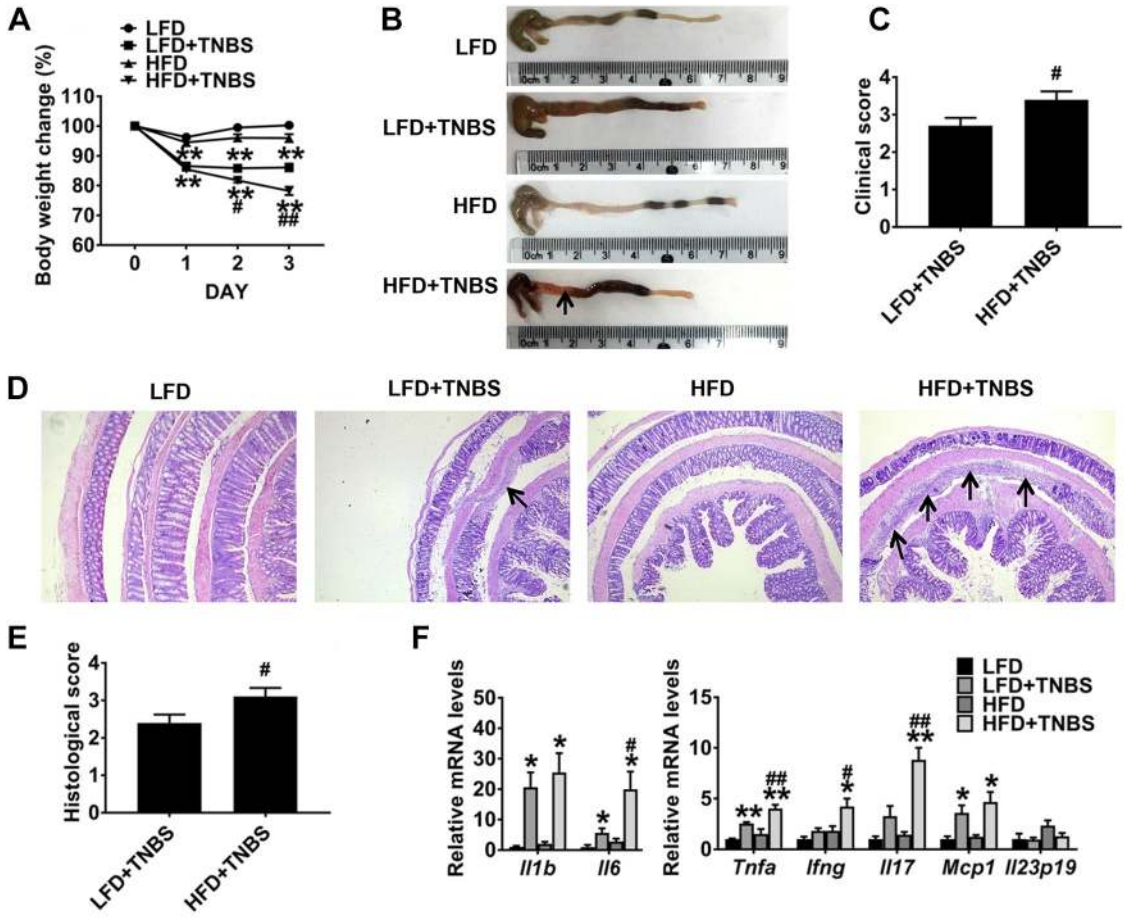

Fig. 2. High-fat diet (HFD) feeding exacerbates colitis in mice. *A*: body weight changes in mice on low-fat diet (LFD) or HFD for 4 wk following 2,4,6-trinitrobenzenesulfonic acid (TNBS) treatment. $^{**}P < 0.01$ vs. respective LFD or HFD; $\#P < 0.05$, $\#\#P < 0.01$ vs. LFD+TNBS; $n = 5$ each group. *B*: gross morphology of the colons on *day 3* after TNBS treatment (arrow points to bleeding). *C*: clinical score of the colons on *day 3* after TNBS treatment. $\#P < 0.05$ vs. LFD+TNBS; $n = 10$ each group. *D*: hematoxylin and eosin histology of the colons on *day 3* after TNBS treatment (arrows point to the ulcerated area; magnification: ×50). *E*: histological score of the colons on *day 3* after TNBS treatment. $\#P < 0.05$ vs. LFD+TNBS; $n = 10$ each group. *F*: real-time RT-PCR quantitation of pro-inflammatory cytokines and chemokines in colonic mucosa on *day 3* after TNBS treatment. $^{*}P < 0.05$, $^{**}P < 0.01$ vs. LFD or HFD; $\#P < 0.05$, $\#\#P < 0.01$ vs. LFD+TNBS; $n = 3$–5 each group.

RT-PCR. Total RNAs were extracted using TRIzol reagent (Invitrogen). First-strand cDNA was synthesized using PrimeScript RT reagent kit (TaKaRa, Mountain View, CA). Real-time PCR was performed using SYBR Premix Ex kit (TaKaRa) in an ABI 7500 real-time system. The relative amounts of transcripts were calculated using the $2^{-\Delta\Delta Ct}$ formula (35), normalized to GAPDH as an internal control. PCR primers are provided in Table 1.

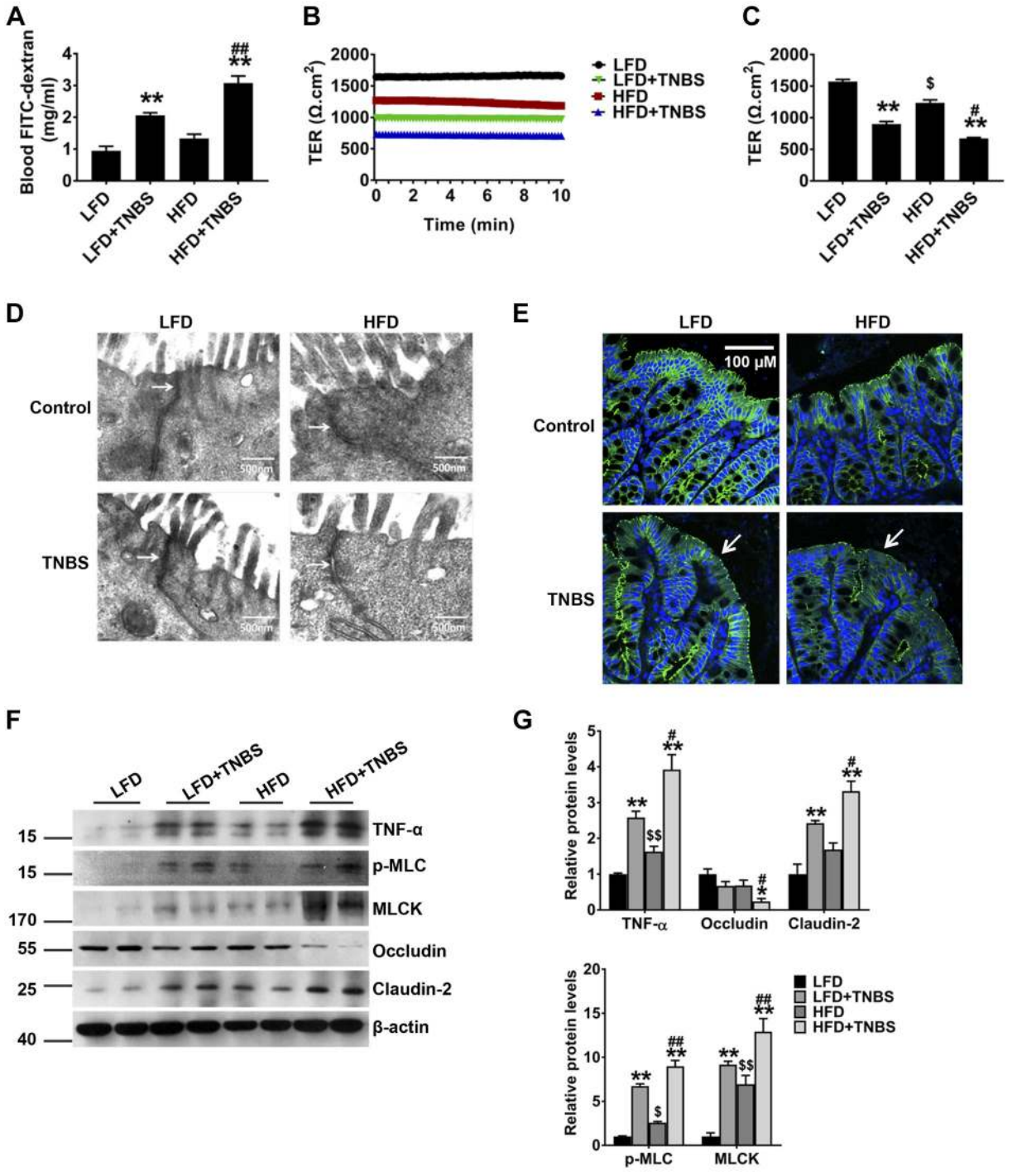

Fig. 3. High-fat diet (HFD) feeding increases the permeability of colonic mucosal barrier. Quantitation of paracellular FITC-dextran passage across mucosal barrier in mice (*A*). $^{**}P < 0.01$ vs. low-fat diet (LFD) or HFD; $^{\#\#}P < 0.01$ vs. LFD+2,4,6-trinitrobenzenesulfonic acid (TNBS); $n = 5$ each group. Ussing chamber assessment (*B*) and quantitation (*C*) of colonic transepithelial resistance (TER) in LFD-fed and HFD-fed mice on *day 3* after TNBS treatment. $^{**}P < 0.01$ vs. LFD or HFD; $\$P < 0.05$ vs. LFD; $^{\#}P < 0.05$ vs. LFD+TNBS; $n = 3$ each group. Electron microscopic examination of tight junction (arrows) in epithelial barrier (*D*). Immunostaining of colonic epithelium with anti-ZO-1 antibody (*E*). Green, ZO-1; blue, DAPI stained nucleus (magnification: ×200). Arrows indicate diminished ZO-1 on the epithelial surface. Western blot analyses (*F*) and densitometric quantitation (*G*) of indicated proteins in colonic mucosal lysates. $^{*}P < 0.05$, $^{**}P < 0.01$ vs. LFD or HFD; $^{\#}P < 0.05$, $^{\#\#}P < 0.01$ vs. LFD+TNBS; $\$P < 0.05$, $\$\$P < 0.01$ vs. LFD; $n = 5$ each group. Only representative blots are shown. MLC, myosin II regulatory light chain; MLCK, myosin light chain kinase

Statistical analysis. Data values were presented as means ± SE. Statistical comparisons were carried out using unpaired two-tailed Student's *t* test for two-group comparisons; for three or more group comparisons, one-way analysis of variance was used with a Student-Newman-Keuls post hoc test. $P < 0.05$ was considered statistically significant.

RESULTS

HFD feeding increases lipid contents in colonic mucosa. To explore the effect of an HFD on the development of colitis, we fed C57BL/6 mice a HFD for 1 mo before subjecting them to the TNBS colitis model. As expected, mice fed the HFD showed a higher rate of body weight increase compared with mice receiving LFD (Fig. 1*A*). At the end of this dietary treatment, the HFD-fed mice exhibited significant increases in plasma triglyceride, cholesterol, and free fatty acid concentrations (Fig. 1, *B–D*). Interestingly, HFD also markedly increased the contents of triglyceride and cholesterol in colonic mucosa compared with LFD (Fig. 1, *D* and *E*). The increase in lipid contents, especially within the colonic mucosa, may render the animals more susceptible to colitis development following TNBS induction.

HFD exacerbates the development of experimental colitis. After TNBS installation, mice developed body weight loss within 3 days, an indicator of colitis development, but body weight loss was more severe in HFD-fed mice compared with LFD-fed mice (Fig. 2*A*). TNBS-treated colons were shortened and swollen, with signs of bleeding and no visible fecal pellet formation (Fig. 2*B*), and semiquantitative evaluation of these colons showed that HFD-fed mice had significantly higher clinical scores than LFD-fed mice (Fig. 2*C*). Histological examination revealed more severe colonic ulceration and histological damage in HFD-fed mice compared with LFD-fed mice following TNBS induction (Fig. 2, *D* and *E*). HFD-fed mice developed much larger ulcerative lesions in the distal colon after TNBS induction (Fig. 2*D*). Moreover, HFD-treated mice expressed much higher levels of pro-inflammatory cytokines and chemokines (TNF-α, IL-1β, IL-6, INF-γ, IL-23p19, IL-17, and MCP-1) in the colonic mucosa compared with LFD-treated mice following TNBS induction (Fig. 2*F*). Together these observations indicate that HFD enhances colonic inflammation and exacerbates colitis development in the TNBS experimental colitis model.

HFD increases colonic mucosal permeability. To explore the mechanism of increased colonic inflammation in HFD-treated mice, we assessed colonic permeability by FITC-dextran gavage and Ussing chamber assays. In FITC-dextran feeding assays, HFD-fed mice exhibited greater increases in plasma FITC-dextran concentrations compared with LFD-treated mice, indicating greater intestinal permeability in HFD-fed mice following TNBS induction (Fig. 3*A*). Direct measurement of colonic mucosal TER using the Ussing chamber

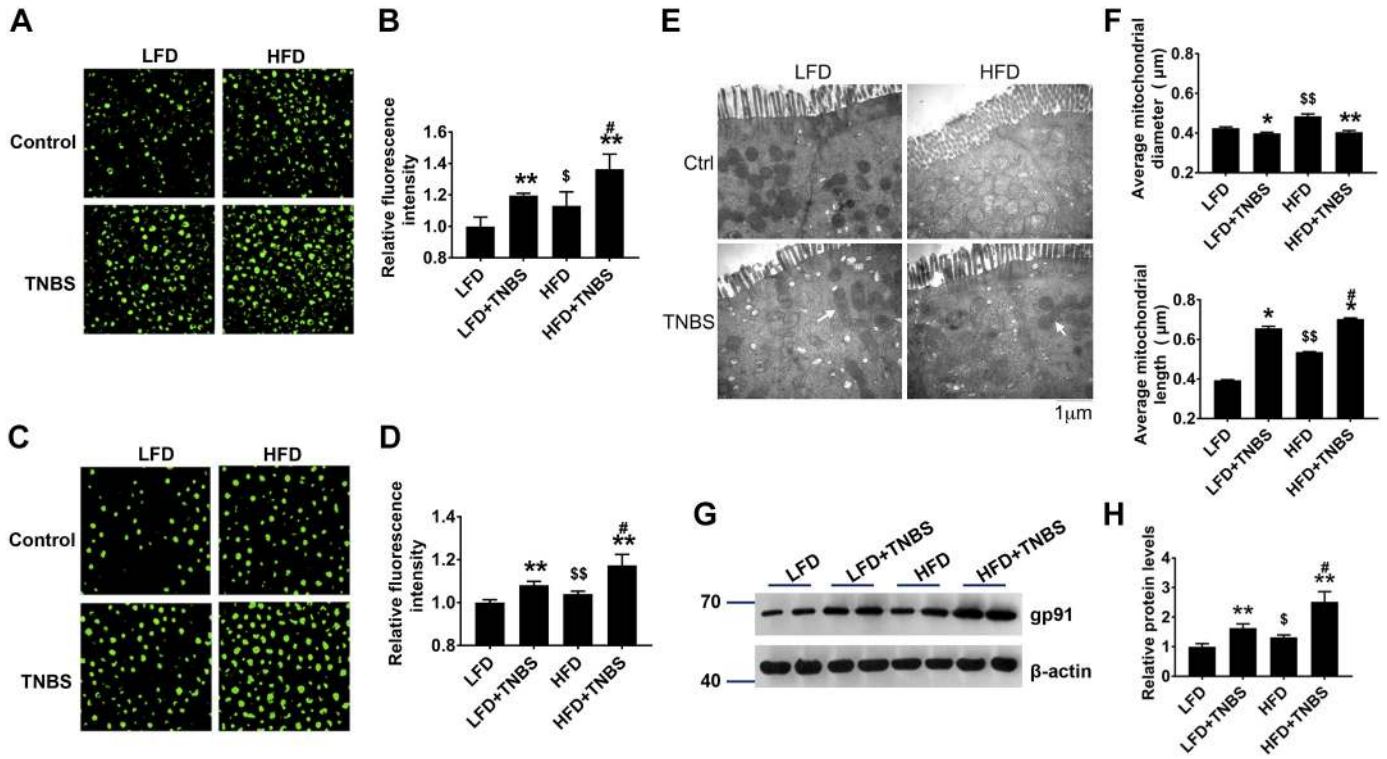

Fig. 4. High-fat diet (HFD) feeding induces oxidative stress in colonic mucosa. Representative images of reactive oxygen species (ROS)-induced dichlorofluorescein fluorescence (*A*) and quantification of ROS production (*B*) in purified colonic epithelial cells (magnification: ×200). $^{**}P < 0.01$ vs. LFD or HFD, $^{\#}P < 0.05$ vs. LFD+2,4,6-trinitrobenzenesulfonic acid (TNBS); $\$P < 0.05$ vs. LFD; $n = 4$ each group. Representative images of ROS-induced dichlorofluorescein fluorescence (*C*) and quantification of ROS production (*D*) in isolated colonic lamina propria cells (magnification: ×200). $^{**}P < 0.01$ vs. LFD or HFD; $\$\$P < 0.01$ vs. LFD; $^{\#}P < 0.05$ vs. LFD+TNBS; $n = 4$ each group. Electron microscopic examination of mitochondrial structure in colonic epithelial cells from the four groups of mice (*E*). Arrows indicate examples of elongated mitochondria. Average mitochondrial diameter (width) and length (*F*). $^{*}P < 0.05$, $^{**}P < 0.01$ vs. LFD or HFD; $\$\$P < 0.01$ vs. LFD; $^{\#}P < 0.05$ vs. LFD+TNBS. Representative Western blot (*G*) and densitometric quantitation (*H*) of gp91. $^{**}P < 0.01$ vs. LFD or HFD; $^{\#}P < 0.05$ vs. LFD+TNBS; $\$P < 0.05$ vs. LFD; $n = 5$ each group.

confirmed that TNBS markedly reduced colonic TER in both HFD-fed and LFD-fed mice, but the reduction in TER was greater in HFD-treated mice (Fig. 3, *B* and *C*). Consistent with these results, electron microscopy revealed a more open tight junction structure in the colonic epithelial barrier of HFD-treated mice following TNBS insult (Fig. 3*D*). Moreover, immunostaining of the mucosal epithelium with anti-ZO-1 antibody revealed marked decreases in tight junction protein ZO-1 on the epithelial surface of TNBS-treated colons, but HFD-fed mice showed more severe ZO-1 reduction (Fig. 3*E*). Analyses of colonic mucosal lysates with Western blotting showed that TNBS treatment induced TNF-α, MLCK, phospho-MLC, and claudin-2, but suppressed occludin, and these changes were more robust in HFD-fed mice (Fig. 3, *F* and *G*). These are well-known markers for intestinal epithelial tight junction dysfunction, largely accounting for the increased permeability of mucosal epithelial barrier. Thus, HFD promotes the disruption of colonic epithelial barrier in this experimental colitis model.

HFD induces oxidative stress in mucosal epithelial cells and lamina propria cells. To better understand how HFD damages the mucosal barrier, we assessed oxidative stress in colonic epithelial cells and lamina propria cells. As shown in Fig. 4, HFD feeding increased ROS production in both colonic epithelial cells and lamina propria cells at baseline; TNBS treatment markedly induced ROS production in these cells, but the induction of ROS was more robust in HFD-fed mice (Fig. 4, *A–D*). Electron microscopic examination showed that HFD feeding increased mitochondrial size and probably induced mitochondrial fusion within colonic epithelial cells, especially in the presence of TNBS (Fig. 4, *E* and *F*), signs of increased cellular stress and mitochondrial overactivation that can lead to increased ROS production (46). TNBS treatment induced the expression of gp91, a key subunit of NADPH oxidase, in colonic mucosa, and HFD feeding further enhanced gp91 expression in the colon (Fig. 4, *G* and *H*). These data indicate that HFD feeding increases oxidative stress in colonic mucosa, which contributes to mucosal barrier injury in experimental colitis.

Fatty acids and pro-inflammatory cytokines induce oxidative stress in colonic epithelial cells. We speculated that high lipid content and inflammation in the mucosa are key factors that promoted epithelial barrier dysfunction. To mimic these factors, we exposed HCT116 colonic epithelial cells to PA, TNF-α, or both. PA is a major long-chain saturated fatty acid that is known to alter cellular metabolism, increase oxidative stress, and promote inflammation (5, 28), and it is the most widely used fatty acid in studying oxidative stress and inflammation. As shown in Fig. 5, either PA or TNF-α treatment was able to induce ROS production in HCT116 cells, and the combination of PA and TNF-α had much greater effects on ROS induction (Fig. 5, *A* and *B*). Moreover, JC-1 assays showed that TNF-α or PA and TNF-α combination induced mitochondrial depolarization, with the combination having

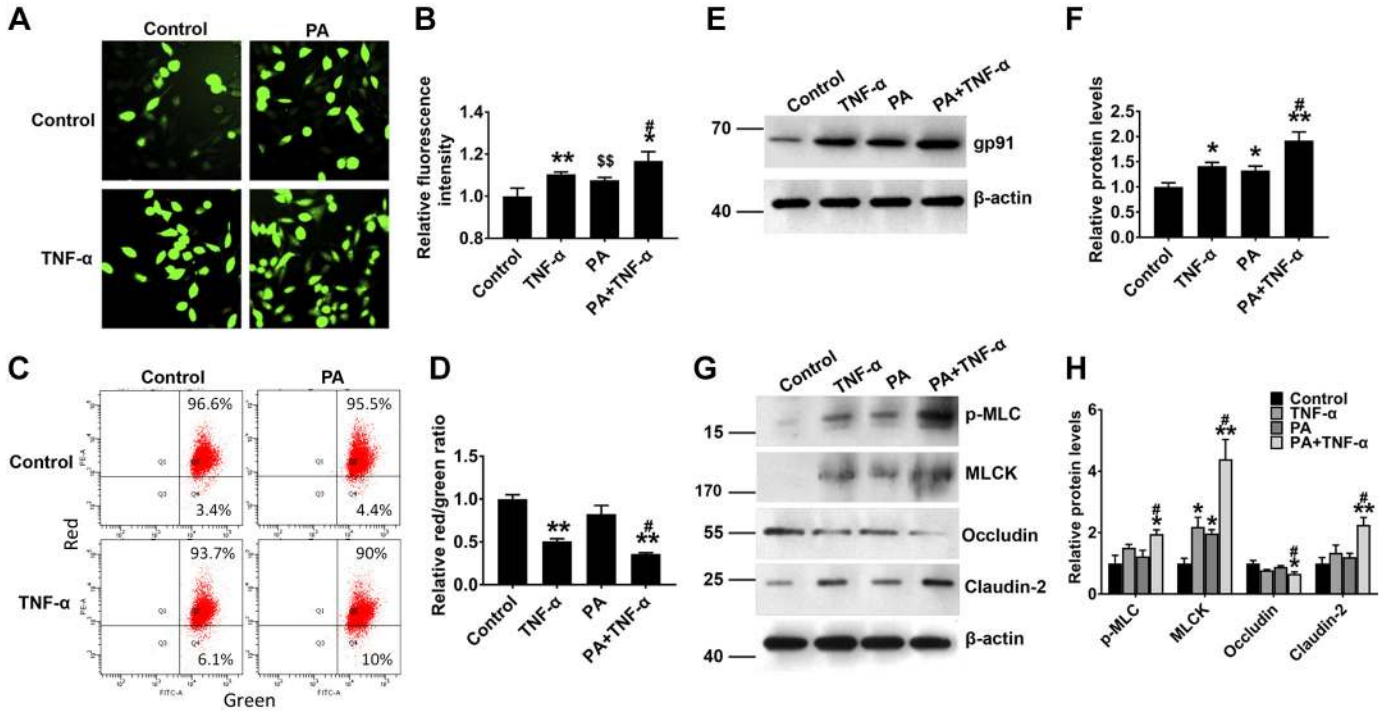

Fig. 5. Fatty acid and pro-inflammatory cytokine induce oxidative stress and activate myosin light chain kinase (MLCK) pathway in colonic epithelial cell line. Representative images of reactive oxygen species (ROS)-induced dichlorofluorescein fluorescence (*A*) and quantification of ROS production (*B*) in HCT116 cells under different treatments as indicated (magnification: ×200). $*P < 0.05$; $**P < 0.01$ vs. Control; $\$\$P < 0.01$ vs. Control; $\#P < 0.05$ vs. palmitic acid (PA) or TNF-α; $n = 4$ each group. Representative flow cytometry plots (*C*) and quantitation of red/green fluorescence ratio (*D*) for HCT116 cells stained with JC-1. $**P < 0.01$ vs. Control; $\#P < 0.05$ vs. PA or TNF-α; $n = 3$ each group. Representative Western blot (*E*) and densitometric quantitation (*F*) of gp91 from the four treatment groups. $*P < 0.05$, $**P < 0.01$ vs. Control; $\#P < 0.05$ vs. PA or TNF-α; $n = 4$ each group. Western blot analyses (*G*) and densitometric quantitation (*H*) of indicated proteins in cell lysates from the four treatment groups. $*P < 0.05$, $**P < 0.01$ vs. Control; $\#P < 0.05$ vs. PA or TNF-α; $n = 3$–5 each group. JC-1, tetraethylbenzimidazolylcarbocyanine iodide.

greater activity to reduce mitochondrial membrane potential (Fig. 5, *C* and *D*), a sign of mitochondrial dysfunction that can lead to ROS overproduction. Consistently, PA or TNF-α alone induced gp91 expression in these cells, but the combination of both had greater inducing effects (Fig. 5, *E* and *F*). Moreover, similar effects of PA, TNF-α, and their combination could be seen on the induction of MLCK, phospho-MLC, and claudin-2 as well as on the suppression of occludin in HCT116 cells (Fig. 5, *G* and *H*). These results infer that fatty acid and inflammation are the key factors driving ROS production and colonic epithelial tight junction dysfunction.

ROS depletion rescues mitochondrial dysfunction and prevents oxidative stress in colonic epithelial cells. To confirm the detrimental effects of ROS production on colonic epithelial cells, we treated HCT116 cells with PA and TNF-α in the presence or absence of NAC, an antioxidant that scavenges ROS inside the cell (10). As shown in Fig. 6, NAC markedly inhibited the production of ROS in HCT116 cells induced by PA and TNF-α (Fig. 6, *A* and *B*). NAC also effectively reduced mitochondrial depolarization induced by PA and TNF-α (Fig. 6, *C* and *D*). Consequently, NAC treatment prevented the induction of MLC phosphorylation and claudin 2 and gp91 expression and the reduction of occludin that were caused by PA and TNF-α cotreatment (Fig. 6, *E* and *F*). These observations suggest that depletion of ROS ameliorates mitochondrial dysfunction and tight junction dysfunction, confirming a role of ROS in mucosal epithelial injury.

Short-term HFD feeding is insufficient to promote colitis. To assess whether HFD feeding per se can promote colitis in the absence of obesity in our model, we fed the mice HFD for 1 wk, when obesity had not yet developed, before subjecting them to the TNBS model. We found that this short-term HFD feeding promoted colitis to some extent, but except for some colonic pro-inflammatory cytokines (IL-1β, MCP-1), most data did not reach significance between LFD-fed and HFD-fed mice (Fig. 7, *A*–*F*). These observations suggest that obesity, particularly obesity-associated inflammation, may be required to promote colitis in our model.

DISCUSSION

Diets high in saturated fats are thought to increase the risk of IBD in humans (38). Moreover, Western diets that contain high n-6 polyunsaturated fatty acid (PUFA) or have unbalanced n-3 PUFA/n-6 PUFA ratio are thought to be IBD promoting, as n-6 PUFAs are pro-inflammatory whereas n-3 PUFAs can counter the effect of n-6 PUFAs (24). Consistent with these views, in this study we showed that HFD feeding exacerbates colitis in an experimental model of colitis, manifested by more robust mucosal inflammation and more severe colonic damage in HFD-fed mice relative to LFD-fed mice. HFD feeding increases lipid contents in colonic mucosa, which we speculate is a key initiating pathogenic factor that alters the microenvironment within the mucosa, enhances cellular metabolism, and induces oxidative stress, setting the stage for epithelial barrier

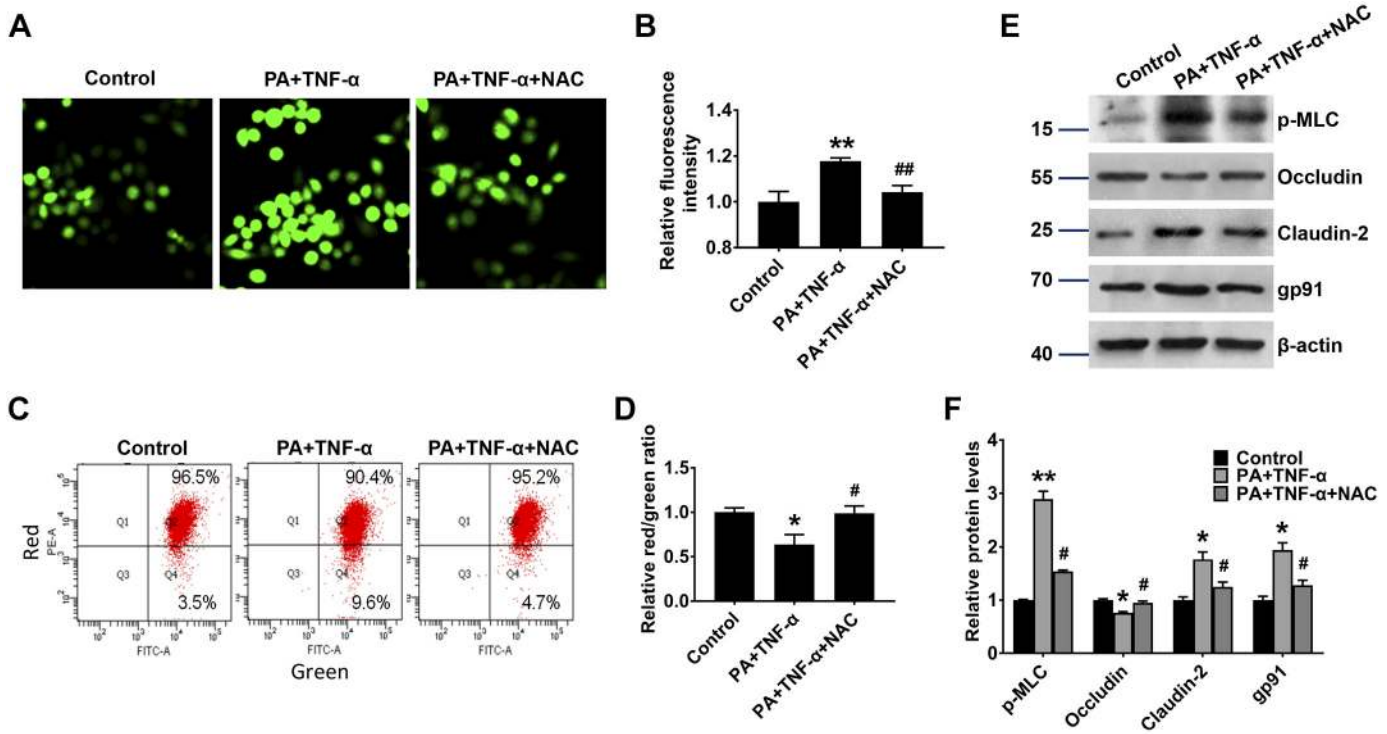

Fig. 6. Reactive oxygen species (ROS) depletion partially rescues mitochondrial dysfunction and prevents oxidative stress and activation of myosin light chain kinase (MLCK) pathway in colonic epithelial cell line. Representative images of ROS-induced dichlorofluorescein fluorescence (*A*) and quantification of ROS production (*B*) in HCT116 cells stained with JC-1 after exposure to PA and TNF-α in the presence or absence of *N*-acetyl-L-cysteine (NAC) (magnification: ×200). $^{**}P < 0.01$ vs. Control; $\#\#P < 0.01$ vs. palmitic acid (PA)+TNF-α; $n = 3$ each group. Representative flow cytometry plots (*C*) and quantitation of red/green fluorescence ratio (*D*) in HCT116 cells under similar treatments. $^{*}P < 0.05$ vs. Control; $\#P < 0.05$ vs. PA+TNF-α; $n = 5$ each group. Western blot analyses (*E*) and densitometric quantitation (*F*) of indicated proteins in HCT116 cells under similar treatments. $^{*}P < 0.05$, $^{**}P < 0.01$ vs. Control; $\#P < 0.05$ vs. PA + TNF-α; $n = 3$ each group. JC-1, tetraethylbenzimidazolylcarbocyanine iodide.

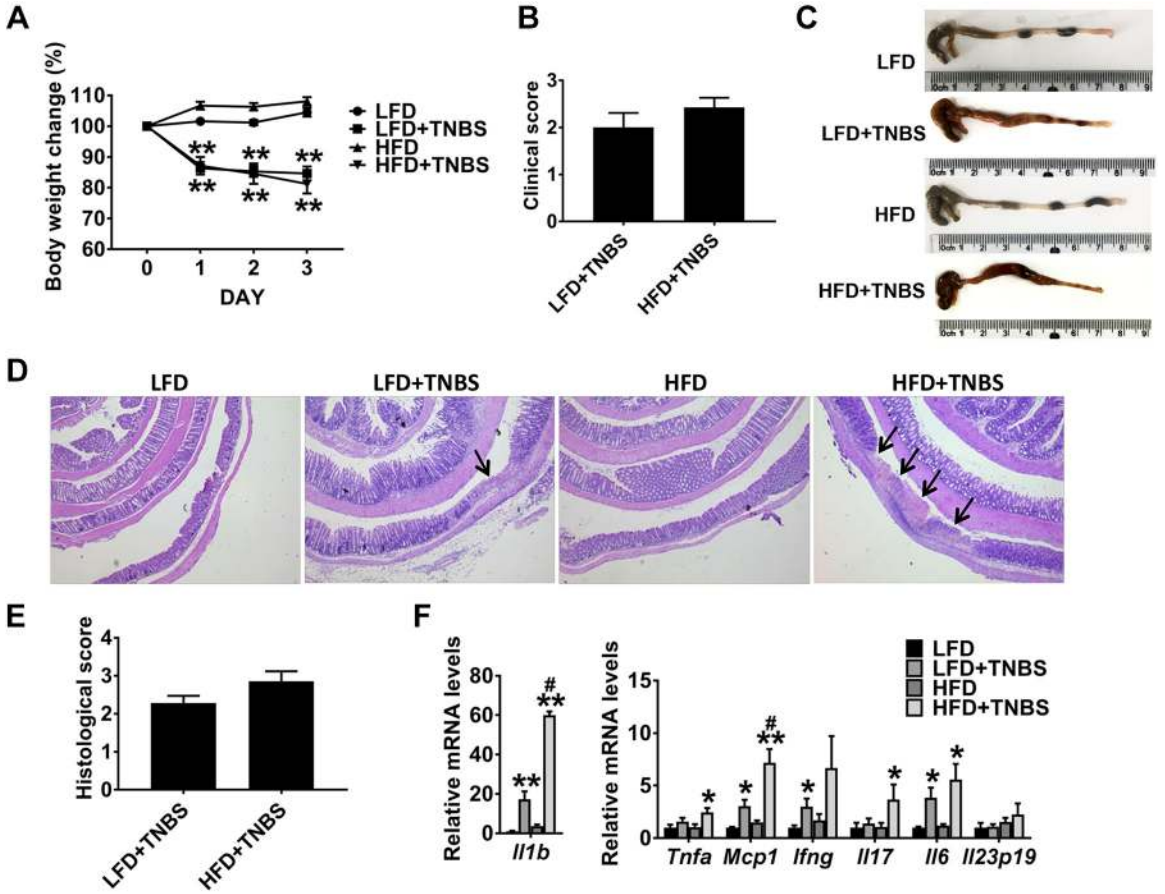

Fig. 7. Effects of short-term high-fat diet (HFD) feeding on the development of experimental colitis. *A*: body weight changes in mice on low-fat diet (LFD) or HFD for 1 wk after 2,4,6-trinitrobenzenesulfonic acid (TNBS) treatment. $^{**}P < 0.01$ vs. respective LFD or HFD; $n = 4$ each group. *B*: clinical score of the colons on *day 3* after TNBS treatment. $n = 7$ each group. *C*: gross morphology of the colons on *day 3* after TNBS treatment. *D*: hematoxylin and eosin histology of the colons on *day 3* after TNBS treatment (arrows point to the ulcerated area; magnification: ×50). *E*: histological score of the colons on *day 3* after TNBS treatment. $n = 7$ each group. *F*: real-time RT-PCR quantitation of pro-inflammatory cytokines and chemokines in colonic mucosa on *day 3* after TNBS treatment. $^{*}P < 0.05$, $^{**}P < 0.01$ vs. LFD or HFD; $\#P < 0.05$ vs. LFD+TNBS; $n = 4$ each group.

dysfunction and thus the development of colonic mucosal inflammation.

There have been a number of prior studies that have demonstrated the detrimental effect of HFD on the development of colitis. For example, Cheng et al. (6) reported that HFD exacerbated colitis through disruption of dendritic cell homeostasis in a dextran sulfate sodium-induced colitis model. Paik et al. (27) showed that HFD-induced obesity exacerbated colitis in genetically susceptible Mdr1a$^{-/-}$ male mice, whereas Gruber et al. (14) demonstrated that HFD feeding accelerated the onset of CD-like ileitis in TNF$^{\Delta ARE/WT}$ mice, which was independent of obesity because this model did not develop obesity. HFD reduced occludin expression and increased intestinal permeability in this model.

In the current study, we set out to explore the effect of HFD on the development of colitis using the TNBS-induced model, which is a model close to CD (26). We showed that mice on HFD developed more severe mucosal inflammation reflected by higher expression of mucosal pro-inflammatory cytokines, and more severe colonic injury reflected by a greater extent of histological abnormalities and mucosal ulceration, as compared with mice on LFD. These observations indicate that HFD indeed promotes colitis. We further presented data showing that HFD feeding disrupted colonic epithelial tight junctions and markedly increased mucosal permeability. At the molecular level, HFD activated the MLCK-MLC pathway that is a major regulator of tight junction permeability (7, 39), reflected by increases in MLCK expression and its substrate MLC phosphorylation. HFD also markedly suppressed occludin and induced claudin-2, two tight junction proteins whose changes here reflected a compromise in the epithelial tight junction structure. Claudin-2 induction is closely associated with mucosal inflammation and IBD (43). We speculate that the molecular basis for HFD to cause these changes lies in its ability to increase oxidative stress in colonic mucosal cells, both epithelial cells and lamina propria cells. We noticed that, even at baseline in the absence of TNBS, HFD feeding increased mitochondrial size and induced ROS production and gp91 expression in these cells; in the presence of TNBS treatment, the effect of HFD on these events was further enhanced. As oxidative stress can induce the production of pro-inflammatory cytokines and directly compromise the mucosal tight junction, we conclude that HFD at least in part exacerbates colitis through inducing oxidative stress in the colonic mucosa.

Our data from in vitro cell cultures support this conclusion. We demonstrated that exposure of colonic epithelial cells to

PA and/or TNF-α disrupted the mitochondrial membrane potential, induced oxidative stress, activated the MLCK-MLC pathway, and altered the expression of tight junction proteins occludin and claudin-2 as seen in mice, and the effect of PA was greatly enhanced in the presence of TNF-α, a major pro-inflammatory cytokine highly produced in colitis in vivo. We also showed that depletion of ROS ameliorated these detrimental effects, confirming the critical role of oxidative stress in epithelial cell injury. These observations suggest that high levels of fatty acids and inflammatory mediators are key factors derived from HFD feeding to drive oxidative stress and disrupt the mucosal barrier integrity.

In our study the mice were fed HFD for 1 mo, which led to the development of obesity. Given that a previous study suggested that obesity is not required for HFD-induced colonic inflammation (14), one important question is whether HFD feeding per se can promote colitis in the absence of obesity in our model. We did actually address this issue by feeding the mice HFD for only 1 wk, when obesity had not yet developed. Although this short-term HFD feeding promoted colitis to some extent, most data did not reach significance between LFD-fed and HFD-fed mice. It is possible that a larger sample size, or longer time, is needed to detect significance, but more likely these observations suggest that obesity, particularly obesity-associated inflammation, is an important pathogenic factor to promote colitis in the TNBS model. This notion is supported by our in vitro observations that TNF-α acts synergistically or additively with PA to promote oxidative stress and tight junction protein dysregulation in colonic epithelial cells (Fig. 5).

IBD was used to be considered as a problem in industrial-urbanized societies and was attributed largely to a Westernized lifestyle and other associated environmental factors, but now the incidence and prevalence of IBD are steadily increasing around the world in both developed and developing countries. The rapid Westernization of the population in developing countries could be a reason for the rising IBD incidence (23). Our study suggests that Western diets, high in saturated fats, can indeed promote or contribute to the risk of IBD. Therefore, dietary factors ought to be carefully considered in the IBD population (24).

GRANTS

This work was supported in part by a research grant from Liaoning Provincial Government.

DISCLOSURES

No conflicts of interest, financial or otherwise, are declared by the authors.

AUTHOR CONTRIBUTIONS

Y.C.L. conceived and designed research; Xue Li, X.W., and Y.S. performed experiments; Xue Li, J.D., Z.X., and Y.C.L. analyzed data; J.D., Xin Li, Z.X., and Y.C.L. interpreted results of experiments; Xue Li and Y.C.L. prepared figures; Xue Li and Y.C.L. drafted manuscript; Y.C.L. edited and revised manuscript; Xue Li, X.W., Y.S., J.D., Xin Li, Z.X., and Y.C.L. approved final version of manuscript.

REFERENCES

1. **Ananthakrishnan AN, Khalili H, Konijeti GG, Higuchi LM, de Silva P, Fuchs CS, Willett WC, Richter JM, Chan AT.** Long-term intake of dietary fat and risk of ulcerative colitis and Crohn's disease. *Gut* 63: 776–784, 2014. doi:10.1136/gutjnl-2013-305304.
2. **Appleyard CB, Wallace JL.** Reactivation of hapten-induced colitis and its prevention by anti-inflammatory drugs. *Am J Physiol Gastrointest Liver Physiol* 269: G119–G125, 1995. doi:10.1152/ajpgi.1995.269.1.G119.
3. **Bligh EG, Dyer WJ.** A rapid method of total lipid extraction and purification. *Can J Biochem Physiol* 37: 911–917, 1959. doi:10.1139/y59-099.
4. **Chazotte B.** Labeling mitochondria with JC-1. *Cold Spring Harb Protoc* 2011: pdb.prot065490, 2011.
5. **Chen Y, Deb DK, Fu X, Yi B, Liang Y, Du J, He L, Li YC.** ATP-citrate lyase is an epigenetic regulator to promote obesity-related kidney injury. *FASEB J* 33: 9602–9615, 2019. doi:10.1096/fj.201900213R.
6. **Cheng L, Jin H, Qiang Y, Wu S, Yan C, Han M, Xiao T, Yan N, An H, Zhou X, Shao Q, Xia S.** High fat diet exacerbates dextran sulfate sodium induced colitis through disturbing mucosal dendritic cell homeostasis. *Int Immunopharmacol* 40: 1–10, 2016. doi:10.1016/j.intimp.2016.08.018.
7. **Clayburgh DR, Rosen S, Witkowski ED, Wang F, Blair S, Dudek S, Garcia JG, Alverdy JC, Turner JR.** A differentiation-dependent splice variant of myosin light chain kinase, MLCK1, regulates epithelial tight junction permeability. *J Biol Chem* 279: 55506–55513, 2004. doi:10.1074/jbc.M408822200.
8. **Cunningham KE, Turner JR.** Myosin light chain kinase: pulling the strings of epithelial tight junction function. *Ann NY Acad Sci* 1258: 34–42, 2012. doi:10.1111/j.1749-6632.2012.06526.x.
9. **Du J, Chen Y, Shi Y, Liu T, Cao Y, Tang Y, Ge X, Nie H, Zheng C, Li YC.** 1,25-Dihydroxyvitamin D protects intestinal epithelial barrier by regulating the myosin light chain kinase signaling pathway. *Inflamm Bowel Dis* 21: 2495–2506, 2015. doi:10.1097/MIB.0000000000000526.
10. **Ezeriņa D, Takano Y, Hanaoka K, Urano Y, Dick TP.** N-acetyl cysteine functions as a fast-acting antioxidant by triggering intracellular H_2S and sulfane sulfur production. *Cell Chem Biol* 25: 447–459.e4, 2018. doi:10.1016/j.chembiol.2018.01.011.
11. **Fasano A, Shea-Donohue T.** Mechanisms of disease: the role of intestinal barrier function in the pathogenesis of gastrointestinal autoimmune diseases. *Nat Clin Pract Gastroenterol Hepatol* 2: 416–422, 2005. doi:10.1038/ncpgasthep0259.
12. **Gangwar R, Meena AS, Shukla PK, Nagaraja AS, Dorniak PL, Pallikuth S, Waters CM, Sood A, Rao R.** Calcium-mediated oxidative stress: a common mechanism in tight junction disruption by different types of cellular stress. *Biochem J* 474: 731–749, 2017. doi:10.1042/BCJ20160679.
13. **Gibson PR.** Increased gut permeability in Crohn's disease: is TNF the link? *Gut* 53: 1724–1725, 2004. doi:10.1136/gut.2004.047092.
14. **Gruber L, Kisling S, Lichti P, Martin FP, May S, Klingenspor M, Lichtenegger M, Rychlik M, Haller D.** High fat diet accelerates pathogenesis of murine Crohn's disease-like ileitis independently of obesity. *PLoS One* 8: e71661, 2013. doi:10.1371/journal.pone.0071661.
15. **He L, Liu T, Shi Y, Tian F, Hu H, Deb DK, Chen Y, Bissonnette M, Li YC.** Gut epithelial vitamin D receptor regulates microbiota-dependent mucosal inflammation by suppressing intestinal epithelial cell apoptosis. *Endocrinology* 159: 967–979, 2018. doi:10.1210/en.2017-00748.
16. **Hyland NP, Chambers AP, Keenan CM, Pittman QJ, Sharkey KA.** Differential adipokine response in genetically predisposed lean and obese rats during inflammation: a role in modulating experimental colitis? *Am J Physiol Gastrointest Liver Physiol* 297: G869–G877, 2009. doi:10.1152/ajpgi.00164.2009.
17. **Kamm KE, Stull JT.** Dedicated myosin light chain kinases with diverse cellular functions. *J Biol Chem* 276: 4527–4530, 2001. doi:10.1074/jbc.R000028200.
18. **Knight-Sepulveda K, Kais S, Santaolalla R, Abreu MT.** Diet and inflammatory bowel disease. *Gastroenterol Hepatol (NY)* 11: 511–520, 2015.
19. **Laukoetter MG, Bruewer M, Nusrat A.** Regulation of the intestinal epithelial barrier by the apical junctional complex. *Curr Opin Gastroenterol* 22: 85–89, 2006. doi:10.1097/01.mog.0000203864.48255.4f.
20. **Lewis JD, Abreu MT.** Diet as a trigger or therapy for inflammatory bowel diseases. *Gastroenterology* 152: 398–414.e6, 2017. doi:10.1053/j.gastro.2016.10.019.
21. **Li YC, Bolt MJG, Cao L-P, Sitrin MD.** Effects of vitamin D receptor inactivation on the expression of calbindins and calcium metabolism. *Am J Physiol Endocrinol Metab* 281: E558–E564, 2001. doi:10.1152/ajpendo.2001.281.3.E558.
22. **Liu W, Chen Y, Golan MA, Annunziata ML, Du J, Dougherty U, Kong J, Musch M, Huang Y, Pekow J, Zheng C, Bissonnette M,**

Hanauer SB, Li YC. Intestinal epithelial vitamin D receptor signaling inhibits experimental colitis. *J Clin Invest* 123: 3983–3996, 2013. doi:10.1172/JCI65842.

23. **M'Koma AE.** Inflammatory bowel disease: an expanding global health problem. *Clin Med Insights Gastroenterol* 6: 33–47, 2013. doi:10.4137/CGast.S12731.
24. **Marion-Letellier R, Savoye G, Ghosh S.** IBD: in food we trust. *J Crohn's Colitis* 10: 1351–1361, 2016. doi:10.1093/ecco-jcc/jjw106.
25. **Meyer TN, Schwesinger C, Ye J, Denker BM, Nigam SK.** Reassembly of the tight junction after oxidative stress depends on tyrosine kinase activity. *J Biol Chem* 276: 22048–22055, 2001. doi:10.1074/jbc.M011477200.
26. **Neurath MF, Fuss I, Kelsall BL, Stüber E, Strober W.** Antibodies to interleukin 12 abrogate established experimental colitis in mice. *J Exp Med* 182: 1281–1290, 1995. doi:10.1084/jem.182.5.1281.
27. **Paik J, Fierce Y, Treuting PM, Brabb T, Maggio-Price L.** High-fat diet-induced obesity exacerbates inflammatory bowel disease in genetically susceptible Mdr1a-/- male mice. *J Nutr* 143: 1240–1247, 2013. doi:10.3945/jn.113.174615.
28. **Palomer X, Pizarro-Delgado J, Barroso E, Vázquez-Carrera M.** Palmitic and oleic acid: the yin and yang of fatty acids in type 2 diabetes mellitus. *Trends Endocrinol Metab* 29: 178–190, 2018. doi:10.1016/j.tem.2017.11.009.
29. **Park CM, Reid PE, Walker DC, MacPherson BR.** A simple, practical 'swiss roll' method of preparing tissues for paraffin or methacrylate embedding. *J Microsc* 145: 115–120, 1987. doi:10.1111/j.1365-2818.1987.tb01321.x.
30. **Podolsky DK.** Inflammatory bowel disease. *N Engl J Med* 347: 417–429, 2002. doi:10.1056/NEJMra020831.
31. **Rao R.** Oxidative stress-induced disruption of epithelial and endothelial tight junctions. *Front Biosci* 13: 7210–7226, 2008. doi:10.2741/3223.
32. **Rao RK, Baker RD, Baker SS, Gupta A, Holycross M.** Oxidant-induced disruption of intestinal epithelial barrier function: role of protein tyrosine phosphorylation. *Am J Physiol Gastrointest Liver Physiol* 273: G812–G823, 1997. doi:10.1152/ajpgi.1997.273.4.G812.
33. **Reuter S, Gupta SC, Chaturvedi MM, Aggarwal BB.** Oxidative stress, inflammation, and cancer: how are they linked? *Free Radic Biol Med* 49: 1603–1616, 2010. doi:10.1016/j.freeradbiomed.2010.09.006.
34. **Salim SY, Söderholm JD.** Importance of disrupted intestinal barrier in inflammatory bowel diseases. *Inflamm Bowel Dis* 17: 362–381, 2011. doi:10.1002/ibd.21403.
35. **Schmittgen TD, Livak KJ.** Analyzing real-time PCR data by the comparative C(T) method. *Nat Protoc* 3: 1101–1108, 2008. doi:10.1038/nprot.2008.73.
36. **Shen L, Black ED, Witkowski ED, Lencer WI, Guerriero V, Schneeberger EE, Turner JR.** Myosin light chain phosphorylation regulates barrier function by remodeling tight junction structure. *J Cell Sci* 119: 2095–2106, 2006. doi:10.1242/jcs.02915.
37. **Shi Y, Liu T, He L, Dougherty U, Chen L, Adhikari S, Alpert L, Zhou G, Liu W, Wang J, Deb DK, Hart J, Liu SQ, Kwon J, Pekow J, Rubin DT, Zhao Q, Bissonnette M, Li YC.** Activation of the renin-angiotensin system promotes colitis development. *Sci Rep* 6: 27552, 2016. doi:10.1038/srep27552.
38. **Statovci D, Aguilera M, MacSharry J, Melgar S.** The impact of Western diet and nutrients on the microbiota and immune response at mucosal interfaces. *Front Immunol* 8: 838, 2017. doi:10.3389/fimmu.2017.00838.
39. **Su L, Nalle SC, Shen L, Turner ES, Singh G, Breskin LA, Khramtsova EA, Khramtsova G, Tsai PY, Fu YX, Abraham C, Turner JR.** TNFR2 activates MLCK-dependent tight junction dysregulation to cause apoptosis-mediated barrier loss and experimental colitis. *Gastroenterology* 145: 407–415, 2013. doi:10.1053/j.gastro.2013.04.011.
40. **van der Logt EM, Blokzijl T, van der Meer R, Faber KN, Dijkstra G.** Westernized high-fat diet accelerates weight loss in dextran sulfate sodium-induced colitis in mice, which is further aggravated by supplementation of heme. *J Nutr Biochem* 24: 1159–1165, 2013. doi:10.1016/j.jnutbio.2012.09.001.
41. **Wang F, Graham WV, Wang Y, Witkowski ED, Schwarz BT, Turner JR.** Interferon-gamma and tumor necrosis factor-alpha synergize to induce intestinal epithelial barrier dysfunction by up-regulating myosin light chain kinase expression. *Am J Pathol* 166: 409–419, 2005. doi:10.1016/s0002-9440(10)62264-x.
42. **Watson AJ, Chu S, Sieck L, Gerasimenko O, Bullen T, Campbell F, McKenna M, Rose T, Montrose MH.** Epithelial barrier function in vivo is sustained despite gaps in epithelial layers. *Gastroenterology* 129: 902–912, 2005. doi:10.1053/j.gastro.2005.06.015.
43. **Weber CR, Nalle SC, Tretiakova M, Rubin DT, Turner JR.** Claudin-1 and claudin-2 expression is elevated in inflammatory bowel disease and may contribute to early neoplastic transformation. *Lab Invest* 88: 1110–1120, 2008. doi:10.1038/labinvest.2008.78.
44. **Weigmann B, Tubbe I, Seidel D, Nicolaev A, Becker C, Neurath MF.** Isolation and subsequent analysis of murine lamina propria mononuclear cells from colonic tissue. *Nat Protoc* 2: 2307–2311, 2007. doi:10.1038/nprot.2007.315.
45. **Wirtz S, Neufert C, Weigmann B, Neurath MF.** Chemically induced mouse models of intestinal inflammation. *Nat Protoc* 2: 541–546, 2007. doi:10.1038/nprot.2007.41.
46. **Youle RJ, van der Bliek AM.** Mitochondrial fission, fusion, and stress. *Science* 337: 1062–1065, 2012. doi:10.1126/science.1219855.